Thermal stress restrained specimen test on fiber enhanced asphalt concrete and thermal stress calculation models

Chunshui Huang[1,2,*], Zhanfeng Zhang[3], Danying Dao[2]

1. College of Civil Engineering, XuChang University, Xuchang 461000, China

2. School of Civil Engineering, ZhengZhou University, Zhengzhou 450000, China

3. Henan Tongsheng House Purchasing Co., Ltd., Zhengzhou 450000, China

   chunshuihuang@163.com

ABSTRACT. *Based on the thermal stress restrained specimen test ("TSRST") on polyester fiber reinforced asphalt concrete content, this paper analyzes the effect of fiber volume fraction and draw ratio on low temperature cracking resistance of asphalt concrete, and establishes calculation models for TSRST parameters with consideration of fiber content characteristic parameter's influence. Through analyzing the features of thermal stress-temperature curve for the complete cooling process on the fiber reinforced asphalt concrete, this paper also establishes models for thermal stress calculation with consideration of fiber content characteristic parameter's influence. the TSRST test result and theoretical analysis show that the fiber content characteristic parameter can comprehensively reflect the effect of fiber volume fraction and draw ratio on the low temperature cracking performance of the asphalt concrete. within the testing range of this paper, the fiber reinforced asphalt concrete demonstrates best performance at fiber volume fraction of 0.35%, draw ratio at 324 and fiber content characteristic parameter at 1.13.*

RÉSUMÉ. *En fonction de test des échantillons retenus avec contrainte thermique (TSRST, le sigle de « Thermal Stress Restrained Specimen Test » en anglais) sur le béton bitumineux à renfort de fibres polyester, cet article analyse l'effet de la fraction volumique et du taux d'étirage des fibres sur la résistance à la fissuration du béton bitumineux et établit des modèles de calcul des paramètres TSRST en prenant en compte de l'influence du paramètre caractéristique de teneur de fibres. Par une analyse des caractéristiques de la courbe thermique de contrainte-température pour le processus de refroidissement complet sur le béton bitumineux à renfort de fibres, cet article établit également des modèles de calcul de la contrainte thermique en tenant compte de l'influence du paramètre caractéristique de teneur de fibres. Le résultat du test TSRST et l'analyse théorique montrent que le paramètre caractéristique de teneur de fibres peut refléter de manière exhaustive l'effet de la fraction volumique et du taux d'étirage de fibre sur les performances de fissuration à basse température du béton bitumineux. Dans la plage de test de cet article, le béton bitumineux à renfort de fibres présente les meilleures performances avec une fraction volumique de fibres de 0,35%, un taux d'étirage de 324 et un paramètre caractéristique de teneur de fibres de 1,13.*

1. Introduction

If there is a sudden drop of environmental temperature, the asphalt concrete pavement may suffer from low temperature cracking when the thermal stress generated in temperature shrinkage process is greater than the maximum tensile ductility, or the temperature deformation is greater than the maximum deformability. Water can penetrate the inside of asphalt concrete mixtures, causing erosion to the mineral aggregate and the bitumen, often resulting in failures and damages of the asphalt concrete pavement. It is therefore of great importance to enhance the resilience to low temperature cracking of asphalt concrete pavement for better performance and quality.

Currently, research on low temperature performance of asphalt concrete mixtures, domestically and globally, mostly adopts testing methods including, the low temperature beam bending test and pre-cut seam bending test (Ge *et al*., 2002), low temperature bending creep test (Hao *et al*., 2000), glass-transition temperature test (Yin *et al*., 2010; Cao *et al*., 2006), low temperature splitting test (Tian, *et al*., 2012), and thermal stress restrained specimen test (TSRST) (Pang, 2006; Feng *et al*., 2008; Chen, 1991; Tan *et al*., 2010; Yu *et al*., 2006; Tian *et al*., 2002; Kanerva *et al*., 1994; Jung and Vinson, 1993; Sebaaly *et al*., 2002; Hao and Liu, 2002).

Fiber reinforced asphalt concrete is increasingly popular for its enhanced performance when used on pavements. Research on low temperature of the fiber reinforced asphalt concrete pavement has achieved some significant outcomes, e.g., reference (Guo *et al*., 2004) analyzed the effect that the amount of fiber added has on the cracking resistance of the asphalt concrete mixtures, reference (Wu and Zhang, 2005) analyzed the performance of polyester fiber reinforced asphalt concrete under low temperature using indicators such as bending strain energy, embrittlement point temperature, low temperature creep rate, and elaborated the theory how fiber reinforced asphalt concrete can have enhanced resilience to cracking under low temperature. But from the previous research, there are some issues remaining to be addressed. For example, currently, there is hardly any report on researching the low temperature cracking resistance of fiber reinforced asphalt concrete using TSRST; or on how the fiber's qualities can affect the low temperature performance of asphalt concrete mixtures is relevant to the fiber volume fraction (volume of fiber against volume of asphalt mixture) and the draw ratio (average length against average diameter of fiber), and how to use proper parameters to comprehensively reflect the effect of fiber volume fraction and the draw ration on the low temperature cracking resistance of the asphalt concrete; as well as how to adopt the TSRST results for the

purpose of establishing models for calculating thermal stress endured by the fiber reinforced asphalt concrete pavement. Therefore, this paper conducts the TSRST tests on polyester fiber reinforced asphalt concrete using parameters of fiber volume fraction and the draw ratio. For purpose of testing, the AC-13F mixture is adopted. This research sets to systematically analyze the low temperature cracking resistance of fiber reinforced asphalt concrete, and uses the fiber content characteristic parameters to comprehensively reflect how fiber volume fraction and the draw ratio can affect the cracking resistance performance of asphalt concrete under low temperature. Based on the analysis of the thermal stress – temperature curve of fiber reinforced asphalt concrete, we establish the models for calculating the thermal stress during the complete process when temperature is reduced until cracking and damage occur to the fiber reinforced asphalt concrete as influenced by the fiber content characteristic parameters.

2. Test methods

Thermal Stress Restrained Specimen Test ("TSRST") was first recommended by SHRP Program as a test method for low temperature performance of the asphalt concrete. Domestically, TSRST is also referred to as the low temperature fracture test. The TSRST test is gaining importance as a test method used in asphalt concrete low temperature performance research because this test simulates the stress that the asphalt concrete pavement is under when environmental temperature changes, and provides a realistic reflection of the cracking resistance of asphalt concrete during temperature shrinkage via four direct indicators, namely, Fracture temperature, Fracture intensity, turning point temperature, and thermal stress-temperature curve.

2.1. Components of TSRST equipment

1—Multifunctional testing machine; 2—Load transducer;
3—Temperature control system;   4—Specimen chuck;
5—Displacement measurement system;
6—Bituminous concrete specimen;   7—Servo motor;
8—Testing machine transmission system;
9—High-low temperature chamber;
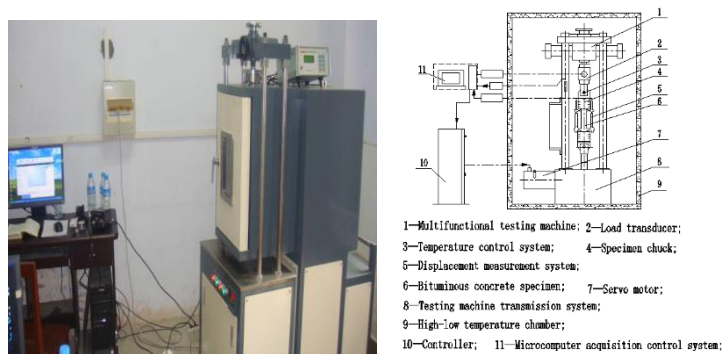10—Controller;   11—Microcomputer acquisition control system;

Figure 1. Tarts equipment

This paper uses a China-made Asphalt Concrete TRST Equipment controlled by computer as shown in Fig 1. This equipment consists of an environmental cabinet with a temperature control range -50°C-+50°C, a multi-function test mainframe, temperature measuring and control system, displacement data collection system, and a computer control and data collection system. The temperature control system maintains a constant temperature control between -50°C-+50°C and enables cooling rate at 5°C/h, 10°C/h, 15°C/h, 20°C/h and 30°C/h. The displacement data collection system collects information on the low temperature deformation the specimen develops along with cooling at a precision rate of 1 μm . The computer control system draws and outputs the thermal stress-temperature curve, thermal stress-time curve, temperature-time curve, and deformation-time curve.

2.2. No-displacement control of tarts test

The key to successful TSRST tests is to keep the length of asphalt concrete specimen unchanged during the cooling process (Pang, 2006; Feng *et al*., 2008; Chen, 1991). For this paper, the China-made TSRST equipment adopts a No-displacement control approach based on "measurement – comparison – compensation" in the process of the TSRST test to avoid any change to the scale distance of specimen (namely the length of specimen measurable by the displacement sensor). The specimen and clamp are placed in the environmental cabinet. Δl_{td} , representing overall deformation of specimen during temperature shrinkage, is the total of the deformation of specimen Δl_{spd} and the deformation of the equipment itself Δl_{syd}. The equation is presented as:

$$\Delta l_{td} = \Delta lspd + \Delta l_{syd}$$

(1)

Before every batch of tests, the room temperature is controlled with air conditioning. Then follow the requirements on the initial temperature and cooling rate for the TSRST test, we use quartz glasses with the same scale distances as shown in Fig 2 to replace the specimen, and produce the curve for quartz glass deformation along with temperature change for the complete cooling process. Taking into consideration that the quartz glass has very little deformation during the temperature shrinkage, we consider this deformation - temperature curve as the system deformation during the cooling process, and input this curve into the control system as the benchmarks. During the tests, the specimen deformation measured is compared against the system deformation as maintained in the system. Therefore, the specimen deformation in the cooling process is presented as:

$$\Delta l_{syd} = \Delta ltd - \Delta l_{syd}$$

(2)

In the case when $\Delta l_{spd} < 0$, the control system sends out stretching instructions and stretch the specimen to its original strength, which means the stretching stops when $\Delta lspd = 0$.
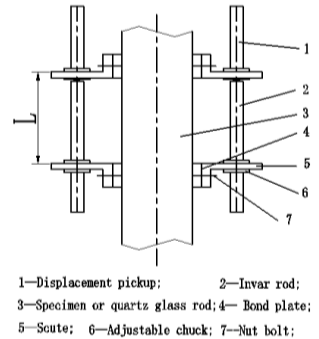
1—Displacement pickup;   2—Invar rod;
3—Specimen or quartz glass rod; 4— Bond plate;
5—Scute;   6—Adjustable chuck; 7—Nut bolt;

Figure 2. Deformation measuring device

During temperature shrinkage, the displacement measuring system constantly measures Δl_{all}, and input the data into the control system. The system conducts comparison and sends out instructions to the servo motor so as to keep the measuring scale distance of the specimen constant. The specimen is under increasing thermal stress until it breaks when its tensile limit is met. This approach provides effective prevention of any effect from the system deformation on test results. But there is also a shortcoming to this approach, in a situation where $\Delta l_{spd} > 0$ as the stretching is controlled with a servo motor, the data collected demonstrates some points that have the same thermal stress levels at different temperatures. As a result, instead of an ideally smooth curve, the thermal stress-temperature curve has serrations or steps. So, we need to export the test data from the control software after completion of the tests, delete the points of the same thermal stresses so that a smooth curve showing relation between thermal stress and temperature can be achieved, and then refer to this curve for the results of TSRST tests.

2.3. TSRST indicators for assessing low temperature performance

This paper provides the results of TSRST as in Fig 3, a thermal stress-temperature curve reflecting the complete cooling process on the fiber reinforced asphalt concrete specimen. This curve directly shows the indicator system for assessing the low temperature performance of fiber reinforced asphalt concrete (Feng *et al*., 2008).

(1) Fracture Temperature T_D: this indicator refers to the temperature at which the specimen, during the cooling process, can no longer endure the increasing thermal stress and break. The Fracture temperature is the lowest temperature the asphalt concrete can bear at a pre-set cooling rate. The lower the Fracture Temperature is, the better the low temperature performance that the fiber reinforced asphalt concrete has.

(2) Fracture Intensity σ_D: The Fracture Intensity is the maximum thermal stress at which the specimen breaks at low temperature. The indicator shows the intensity features of the fiber reinforced asphalt during temperature shrinkage. The higher the

fracture intensity is, the better the low temperature performance that the fiber reinforced asphalt concrete has.

(3) Turning point temperature T_Z: from Fig 3, we can see that at the beginning stage of cooling, the fiber reinforced asphalt concrete displays viscoelasticity. As the temperature keeps dropping, the thermal stress has slow growth rate. The relation between the thermal stress and the temperature is displayed as in a curve, showing the stress relaxation features of the fiber reinforced asphalt concrete. This stage is referred to as the stress relaxation stage; following that, there is a clear turning point of the thermal stress-temperature curve, which is proceeded by some clear elastic patterns. These patterns indicate that thermal stress, along with the reduction of temperature, has rapid growth. This part of the curve is presented via something close to a straight line. There is no relaxation feature to the thermal stress, hence the non-stress relaxation stage. The temperature corresponding to the separation point of stress relaxation stage and the non-stress relaxation stage from thermal stress – temperature curve is the turning point temperature. The lower the turning point temperature is, the better the deformation capacity of the fiber reinforced asphalt concrete has during temperature shrinkage, and the better its cracking resistance performance is.
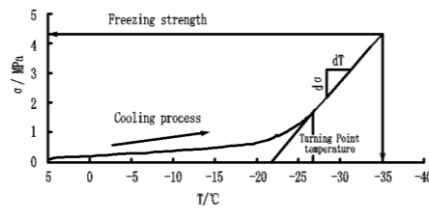

Figure 3. Relationship between thermal stress and temperature

(4) Thermal stress-temperature curve slope K_D: during the non-stress relaxation stage, the thermal stress-temperature curve is close to a straight line. The slope of this line $d\sigma / dT$ is the slope of the thermal stress-temperature curve. This indicator reflects the rate at which the thermal stress endured by the fiber reinforced asphalt concrete grows with the reduction of temperature. The lower the slope is, the slower the thermal stress grows as the temperature decrease during temperature shrinkage for the fiber reinforced asphalt concrete, and the better its cracking resistance performance is.

3. Materials and specimen

Mineral aggregates made in Zhengzhou, No. 70 pavement petroleum asphalt and polyester fiber are used in the TSRST tests. Their performance parameters are listed in Table 1 and Table 2 below. In order to find out the effect of volume fraction and draw ratio of fiber on the test results, we take fibers with draw ratios R_a at 162, 468 and 649 at a volume fraction at 0.35%; while for polyester fibers with a draw ratio R_a

at 324, we take volume fraction rates V_f at 0.17%, 0.35%, 0.52%, and 0.69%. The aggregates are screened, rinsed, and dried before mixed with limestone mineral power to make the AC-13F type median graduation. By use of standard Marshall test, we identify and determine the OAC for regular asphalt concrete mixture and fiber reinforced asphalt concrete mixtures at different levels of fiber volume fractions and draw ratios. The results are listed in Table 3. The next step, the OAC asphalt concrete boards are rolled out and made at dimensions of 300mm×300mm×50mm. The boards are then cut out in 220mm×40mm×40mm for specimens.

Table 1. Properties of aggregates and bituminous

Type of Materials							
Aggregates				Bituminous			
Grain Size /mm	Density /(g/cm^3)	Crushing Value /%	Los Angeles Abrasiveness /%	25°C Penetration /0.1mm	25°C Ductility /cm	Softening Point /°C	Density /(g/cm^3)
16~13.2	2.899	22	23	85	≥100	44.3	1.00937
13.2~9.5	2.905	23	25				
9.5~4.75	2.921	24	26				
4.75~2.36	2.783	/	/				
2.36~1.18	2.647	/	/				
1.18~0.6	2.616	/	/				
0.6~0.3	2.626	/	/				
0.3~0.15	2.627	/	/				
0.15~0.075	2.684	/	/				
0.075~0	2.670	/	/				

Table 2. Properties of polyester fiber

Type of Fiber	Average Length/ mm	Average Diameter/ μm	Draw Ratio	Density/(g/cm^3)	Color	Melting Point/ °C	Tensile Ductility/ MPa
Polyester Fiber	3	18.5	162	1.38	Natural color	255-260	≥500

The results show (Tian *et al*., 2002) that when temperature is above 5℃, the asphalt concrete specimen demonstrates stronger stress-relaxation features, and as a result, it does not show significant enhancing of thermal stress during the cooling process. For purpose of the TSRST test, the initial temperature is set at 5℃ and cooling rate at 10℃/h. The test uses three specimens as a group, fixes the specimens to the clamps using epoxy resin and curing agent mixed at a ratio 1:1, and keeps them in the environmental cabinet for 24 hours set at 5℃ before the specimens are amounted. The environmental cabinet for the TSRST Equipment as shown in Fig 1 is kept for 1 hour at the initial temperature and preloaded with 0.1MPa before the TSRST test is started. Every 10 seconds during the test, data is collected. See Fig 4 for thermal stress-temperature curves for different volume fractions and draw ratios and see Table 4 for the TSRST parameters as results of the thermal stress-temperature curve.

Table 3. Contents of bituminous

Type of Mixtures	Fiber Draw Ratio	Fiber Volume Fraction/%	OACmin/%	OACmax/%	OAC/%
AC-13F	0	0	4.75	5.58	5.32
PFAC-13F	162	0.35	5.88	6.56	6.21
	324	0.17	5.19	5.75	5.41
		0.35	6.30	6.50	6.37
		0.52	5.88	6.48	6.25
		0.69	5.33	6.12	5.93
	486	0.35	5.38	6.06	5.89
	649	0.35	5.42	6.06	5.87

4. Effect of fiber on low-temperature crack resistance performance of asphalt concrete

From Fig 4 and Table 4, we see that the fracture temperature and turning point temperature both have a pattern of going down first before going up along with higher fiber volume fraction and draw ratios. The minimum value is achieved when fiber volume fraction is at 0.35% and draw ratio at 324. The facture intensity, along with higher fiber faction and draw ratios, goes up and then goes down, and achieves its maximum value when fiber volume fraction is at 0.35% and draw ratio at 324. After the turning point temperature, the slope of the thermal stress-temperature curve, along with higher fiber volume fractions and draw ratios, goes down first and then goes up, and also achieves its minimum value when fiber volume fraction is at 0.35% and draw ratio at 324. The results of TSRST on fiber reinforced asphalt concrete show that: a proper amount of fiber can improve the low temperature performance of asphalt concrete; with the fiber type and test conditions adopted in our TSRST test, when fiber volume fraction is at 0.35% and draw ratio at 324, fiber has the best performance-

enhancing effect on the low temperature cracking resistance of asphalt concrete. With overly high fiber volume fraction, overly high or low draw ratio, fiber will undermine the cracking resistance performance of asphalt concrete. The underlying reason is that a proper amount of fiber, when evenly mixed with the asphalt concrete, forms three-dimension fiber grid. During the temperature shrinkage process, the tensile stress on the fibers deters the deformation process. In the meantime, fiber infiltrates, absorbs, and even forms chemical bonding with the acid resin content in the asphalt. In this way, the asphalt film structure is enhanced and thickened, temperature sensibility of asphalt attenuated, and the overall strength of asphalt concrete enhanced. During the temperature shrinkage process with the total length of asphalt concrete specimen kept unchanged, the turning point temperature and fracture temperature are significantly lowered, the slope of thermal stress-temperature curve after the turning point temperature is reduced, and the fracture intensity is notably higher. In addition, the effect that fiber has on asphalt concrete's performance under low temperature is relevant to the density of fiber grid. When the fiber draw ratio is set, within the adequate range of fiber volume fractions, the higher the fiber volume fraction is, the higher the density of the fiber grid, and the better the enhancing effect is. But when the fiber volume fraction is overly high, soft fibers have poorer dispersion, and the fibers that are not evenly disperse can fail to form clusters, while in the meantime, at some parts, the fiber grid forms fiber bundles where the density is too high. The bundled or clustered fiber loses its enhancing effect, and becomes the "flaw" where the stress concentrates during temperature shrinkage on the asphalt concrete. This is the reason why, for fiber asphalt concrete at a fiber volume fraction at 0.69%, the specimen has witnessed lower fracture intensity, higher turning point temperature and fracture temperature, as well as higher slope of the thermal stress-temperature curve. When the fiber volume fraction is pre-set, the fiber draw ratio is another determining element influencing the density of fiber grid. If the fiber diameter is fixed, the lower the draw ratio is, the higher the number of fibers contained in the asphalt concrete base per unit, and higher the density of fiber grid is. The fiber grid, at some parts of the asphalt concrete, clusters when the density is too high. The clustered fibers, forming "flaws" in the asphalt concrete, concentrates the stress during temperature shrinkage. Also, with shorter fiber, the fiber enhancing effect is undermined due to that a single fiber undertakes lower tensile stress during cooling. The higher the fiber draw ratio, the longer a single fiber is. On one hand, if fiber is too long, it breaks since the tensile stress is too high, and on the other hand, it tends to curl and clot due to poorer directivity, therefore leading to undermined enhancing-effect of fibers.
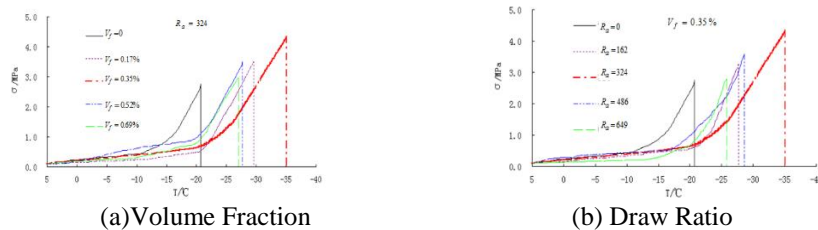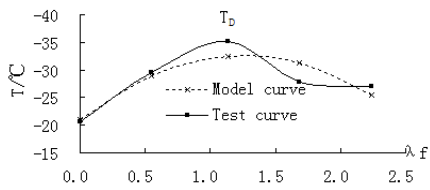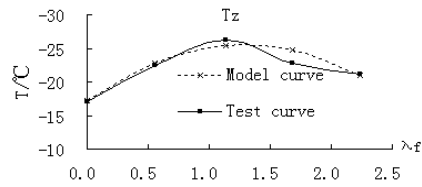

(a) Volume Fraction   (b) Draw Ratio

Figure 4. TSRST results of fiber reinforced asphalt content

Table 4. Test results of TSRST

| Type of Mixture	Fiber Volume Fraction /%	Fiber Draw Ratio	Fracture Temperature /°C	Turning Point Temperature /°C	lope	Fracture Intensity /MPa
AC-13F	0	0	-20.7	-17.0	-0.39	2.73
PFAC-13F	0.35	162	-27.7	-23.2	0.37	3.26
	0.17	324	-29.6	-22.5	-0.36	3.51
	0.35		-35.1	-26.3	-0.32	4.31
	0.52		-27.7	-22.8	-0.37	3.49
	0.69		-27.0	-21.2	-0.41	2.81
	0.35	486	-28.6	-23.9	-0.36	3.57
	0.35	649	-25.8	-21.4	-0.38	2.80

(a)Fracture Temperature

(b)Turning Point Temperature
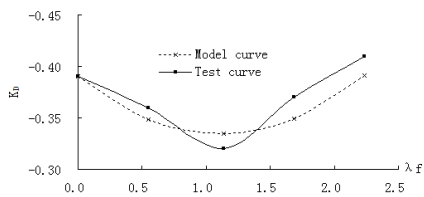
(c) Slope
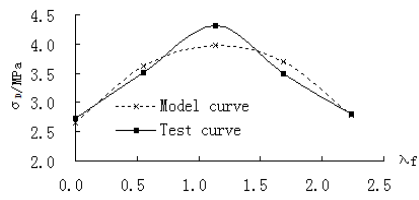
(d) Fracture Intensity

Figure 5. Relationship between TSRST results and fiber content characteristic parameter

Based on the above, fiber volume fraction and draw ratio make important elements to the cracking resistance performance of asphalt concrete content. The fracture temperature T_D, turning point temperature T_Z, fracture intensity σ_D, and the thermal stress-temperature curve slope R_D after the turning point temperature all demonstrate the same change patterns along with the fiber volume fraction and draw ratio. The fiber content characteristic parameters $\lambda_f = V_f \times R_a$ can comprehensively show the effect of fiber volume fraction and draw ratio. From the test results, with consideration of influence of the fiber content characteristic parameters, the relation between fiber content characteristic parameter λ_f and the fracture temperature $T_D(\lambda_f)$, the turning point temperature $T_Z(\lambda_f)$, the fracture intensity $\sigma_D(\lambda_f)$, and the after-turning-point thermal stress-temperature curve slope $K_D(\lambda_f)$ are expressed as below:

$$T_D(\lambda_f) = -20.94 - 18.60\lambda_f + 7.40\lambda_f^2 \tag{5}$$

$$T_Z(\lambda_f) = -17.17 - 12.89\lambda_f + 5.00\lambda_f^2 \tag{6}$$

$$\sigma_D(\lambda_f) = 2.65 + 2.32\lambda_f - 1.01\lambda_f^2 \tag{7}$$

$$K_D(\lambda_f) = -0.39 + 0.10\lambda_f - 0.045\lambda_f^2 \tag{8}$$

Results of calculation from Equation (5) to Equation (8) and the comparison against the TSRST results are shown in Fig 5. It is clear that when fiber content characteristic parameter is at 1.13, the TSRST result for fiber reinforced asphalt concrete has the lowest fracture temperature and turning point temperature, the lowest after-turning-point thermal stress-temperature curve slope, and highest facture intensity. Here the fiber reinforced asphalt concrete demonstrates the best low temperature cracking resistance performance.

5. Model for calculating fiber asphalt concrete thermal stress

The TSRST results show that there are two stages of the cooling process for fiber reinforced concrete specimen, the stress-relaxation stage and non-stress relaxation stage, as shown in Fig 4. When cooling first starts, the fiber reinforced asphalt concrete displays viscoelasticity. As the temperature keeps dropping, the thermal stress has lower growth rate. The relation between the thermal stress and the temperature is displayed in a curve, showing the stress relaxation features of the fiber reinforced asphalt concrete. This stage is referred to as the stress relaxation stage; following that, there is a clear turning point of the thermal stress-temperature curve, which is proceeded by clear elastic patterns. These patterns indicate that thermal stress, along with the decrease of temperature, has rapid growth. This part of the curve is represented via something close to a straight line. There is no relaxation feature to the thermal stress, hence the non-stress relaxation stage. So, during the cooling process,

the thermal stress-temperature curve for fiber reinforced asphalt concrete should meet the following boundary conditions:

$$T = T_0 \, , \, \sigma(T) = a_0 \tag{9}$$

$$|T| = |T_Z(\lambda_f)| \, , \, \frac{d\sigma}{dT} = K_D(\lambda_f) \tag{10}$$

$$|T| = |T_D(\lambda_f)| \, , \, \sigma(T) = \sigma_D(\lambda_f) \tag{11}$$

In this equation: a_0 stands for initial pre-loaded stress; T_0 stands for initial testing temperature.

Thermal stress – temperature model is expressed as:

$$\sigma(T) = \begin{cases} a_0, T = T_0 \\ a + bT + cT^2 + dT^3, T_0 < |T| \le |T_Z| \\ e + K_D T, |T_Z| \le |T| \le |T_D| \end{cases} \tag{12}$$

Table 5. Model parameters of equation (12)

Type of Mixture	Fiber Volume Fraction/%	Fiber Draw Ratio	a	b	c	d	R^2
AC-13F	0	0	0.1459	-0.0166	-0.00050	-0.000200	0.99501
PFAC-13F	0.35	162	0.2471	-0.0254	-0.00367	-0.000182	0.94046
	0.17	324	0.2304	-0.0208	-0.00363	-0.000180	0.94706
	0.35		0.2795	-0.0321	-0.00377	-0.000170	0.98538
	0.52		0.2702	-0.0312	-0.00309	-0.000190	0.96028
	0.69		0.1569	-0.0116	-0.00283	-0.000210	0.98644
	0.35	486	0.2759	-0.0317	-0.00306	-0.000185	0.99087
	0.35	649	0.1811	-0.0150	-0.00288	-0.000190	0.99002

For the stress-relaxation stage of the thermal stress-temperature curve, based on the TSRST results, we use the non-linear fitting available from software Origin8.5, and import the thermal stress-temperature data collected from the test. Base on Equation 12, and assumption of the initial value of model parameters, through adjusting the model parameters, we arrive at the optimal fitting between the theoretical calculation result using the models and the actual test results, and in this way, determine the parameters for Equation 12. The non-linear fitted TSRST test data and model parameters resulted from Equation 12 are shown in Table 5.

From Table 5, we see that Equation 12 model parameter a, as the volume fraction and draw ratio of fiber grow, goes up first and then goes down. When volume fraction is at 0.35% and draw ratio at 324, it reaches the maximum value; parameters b, c, and d, as the volume fraction and draw ratio of fiber grow, go down first and then go up. When volume fraction is at 0.35% and draw ratio at 324, they reach the minimum values. As the fiber volume fraction and draw ratio exert the same patterns of effect on Equation 12, we can use the equation $\lambda_f = V_f \times R_a$ to reflect the effect. The nonlinear fitting Equation (12)'s relation with fiber content characteristic parameter λ_f is expressed as:

$$a(\lambda_f) = 0.1422 + 0.2387\,\lambda_f - 0.0997\,\lambda_f^2 \tag{13}$$

$$b(\lambda_f) = -0.0145 - 0.0303\,\lambda_f + 0.0133\,\lambda_f^2 \tag{14}$$

$$c(\lambda_f) = -0.00087 - 0.00456\,\lambda_f + 0.0017\,\lambda_f^2 \tag{15}$$

$$d(\lambda_f) = -1.99 \times 10^{-4} + 4.58 \times 10^{-5}\,\lambda_f - 2.1 \times 10^{-5}\,\lambda_f^2 \tag{16}$$
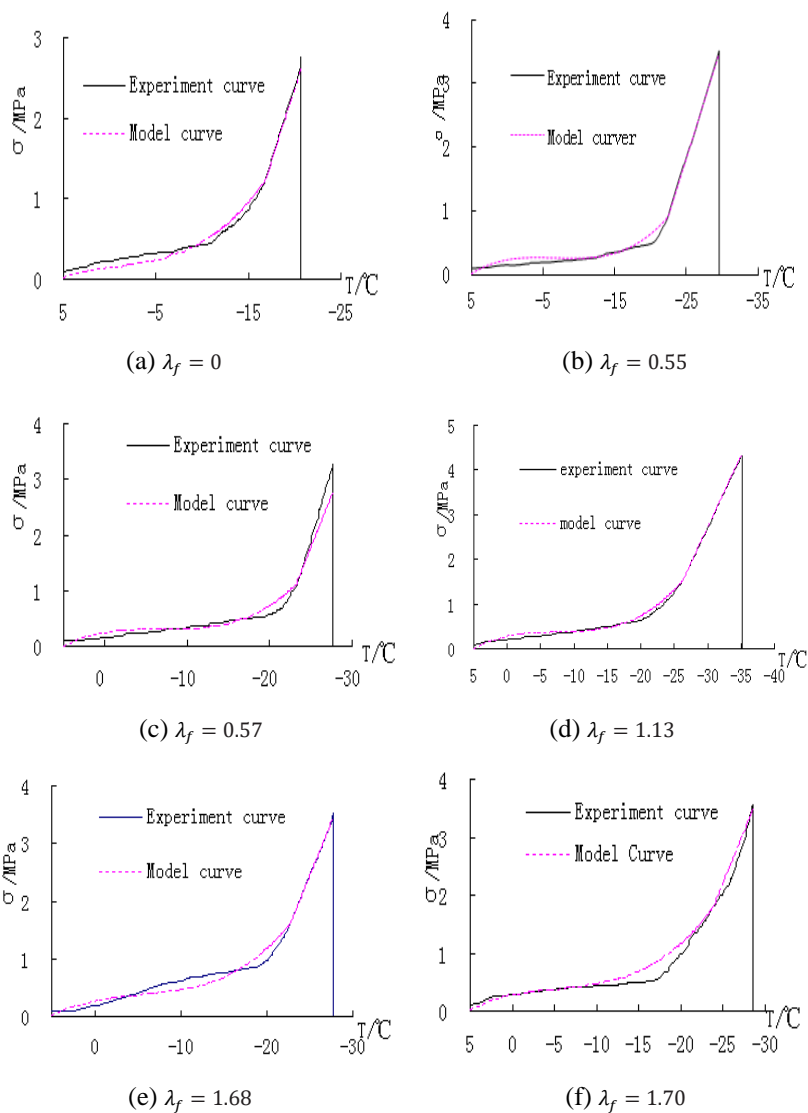
For the non-stress relaxation stage of the thermal stress-temperature curve, when the boundary conditions are adopted, we arrive at a thermal stress-temperature model $e(\lambda_f)$ with consideration of that effect of fiber content characteristic parameters on the asphalt concrete as:

$$e(\lambda_f) = \sigma_D(\lambda_f) - K_D(\lambda_f) \times \left[T_D(\lambda_f) - T_0\right] \tag{17}$$

The thermal stress-temperature model with consideration of the effect of fiber content characteristic parameters on the asphalt concrete can be expressed as below when substituting Equation (13) – (17) into Equation (12):

$$\sigma(T) = \begin{cases} a_0, T = T_0 \\ a(\lambda_f) + b(\lambda_f)T + c(\lambda_f)T^2 + d(\lambda_f)T^3, T_0 < |T| \leq |T_Z| \\ e(\lambda_f) + K_D T, |T_Z| \leq |T| \leq |T_D| \end{cases} \tag{18}$$

When the fiber content characteristic parameter is at 0 (regular asphalt concrete), 0.55 (fiber volume fraction at 0.17%, draw ratio at 324), 0.57 (fiber volume fraction at 0.35%, draw ratio at 162), 1.13 (fiber volume fraction at 0.35%, draw ratio at 324), 1.68 (fiber volume fraction at 0.52%, draw ratio at 324), 1.70 (fiber volume fraction at 0.35%, draw ratio at 468), 2.24 (fiber volume fraction at 0.68%, draw ratio at 324), and 2.27 (fiber volume fraction at 0.35%, draw ratio at 649), the TSRST results and model-calculated results are expressed in curves in Fig 6. We find a good correlation between the thermal stress results calculated from Equation (18) and the TSRST results on fiber reinforced asphalt concrete during cooling.
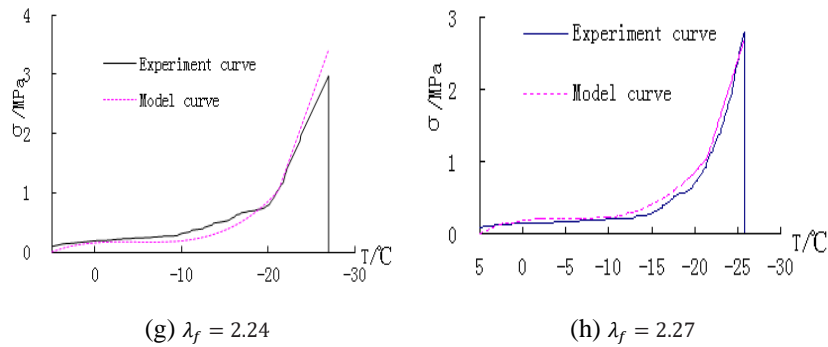
(a) $\lambda_f = 0$

(b) $\lambda_f = 0.55$

(c) $\lambda_f = 0.57$

(d) $\lambda_f = 1.13$

(e) $\lambda_f = 1.68$

(f) $\lambda_f = 1.70$

(g) $\lambda_f = 2.24$ (h) $\lambda_f = 2.27$

Figure 6. Comparison of TSRST curves and model curves

6. Conclusion

(1) The TSRST, as a test method, provides direct reflection of the cracking resistance performance of fiber reinforced concrete under low temperature, with parameters of fracture temperature, fracture intensity, turning point temperature, and slope.

(2) The fiber volume fraction and draw ratio are important elements that determine the low temperature cracking resistance performance of asphalt concrete. The fiber content characteristic parameter can comprehensively reflect the effect of fiber volume fraction and draw ratio on the low temperature cracking resistance of the fiber reinforced asphalt concrete. The results of TSRST demonstrate that when the polyester fiber has a volume fraction at 0.35%, draw ratio at 324, and fiber content characteristic parameter at 1.13, the asphalt concrete has the best cracking resistance performance under low temperature.

(3) The TSRST test results show that there are two stages of the cooling process for fiber reinforced concrete specimen, the stress-relaxation stage and non-stress relaxation stage, divided by the turning point temperature. The stress-relaxation stage has polynomial change features to the thermal stress along with reduction of temperature, while during the non-stress relaxation stage, the thermal stress and temperature have a linear variation pattern. Thermal stress on the fiber reinforced asphalt concrete during the complete process of cooling, with consideration of effect of the fiber content characteristic parameters, can be calculated using Equation (18) model. The model results demonstrate good correlation to the test results.

Reference

Cao L. P., Tan Y. Q., Dong Z. J., Sun L. J. (2006). Evaluation for low temperature performance of SBS modified asphalt using glass transition temperature. *China Journal of Highway and Transport*, Vol. 19, No. 2, pp. 1-6. http://doi.org/10.3321/j.issn:1001-7372.2006.02.001

Chen H. X., Zhang Z. Q., Hu C. S. (2004). Low-temperature anti-cracking performance of fiber-reinforced asphalt mixture. *Journal of South China University of technology (Natural Science Edition)*, Vol. 32, No. 4, pp. 82-86. http://doi.org/10.3321/j.issn:1000-565X.2004.04.019

Chen J. W. (1991). TSRST for asphalt concrete. *Petroleum Asphalt*, Vol. 1, No. 1, pp. 46-50.

Feng K., Xu S. F., Zhang L. B., Li P. (2008). Evaluation of low temperature cracking resistance of asphalt mixtures by means of TSRST method. *Journal of Highway and Transportation Research and Development*, Vol. 25, No. 9, pp. 83-86.

Ge Z. S., Huang X. M., Xu G. G. (2002). Evaluation of asphalt-mixture's low-temperature anti-cracking performance by curvature strain energy method. *Journal of Southeast University (Natural Science Edition)*, Vol. 34, No. 4, pp. 653-655. http://doi.org/10.3321/j.issn:1001-0505.2002.04.026

Guo N. S., Zhao Y. H. (2004). Anti-cracking mechanism of asphalt concrete reinforced by polyester fibers under low temperature. *Highway,* No. 12, pp. 108-111. http://doi.org/10.3969/j.issn.0451-0712.2004.12.027

Guo N. S., Zhao Y. H., Li G. (2004). Analysis of anti-cracking performance of asphalt concrete reinforced by polyester fibers under low temperature. *Journal of Shenyang Arch. And Civ. Eng. Univ*, Vol. 20, No. 1, pp. 1-3. http://doi.org/10.3969/j.issn.2095-1922.2004.01.001

Hao P. W., Liu Z. L. (2002). Study on thermal stress restrained specimen test of asphalt mixture. *Petroleum Asphalt*, Vol. 16, No. 1, pp. 9-11. http://doi.org/10.3969/j.issn.1006-7450.2002.01.002

Hao P. W., Zhang D. L., Hu X. N. (2000). Evaluation method for low temperature anti-cracking performance of asphalt mixture. *Journal of Xi'an Highway University*, Vol. 20, No. 3, pp. 1-5. http://doi.org/10.3321/j.issn:1671-8879.2000.03.001

JTJ 052-2011. Standard test methods of bitumen and bituminous mixtures for highway engineering. *Beijing: China Communications Press*.

Jung D., Vinson T. S. (1993). Thermal stress restrained specimen test to evaluate low-temperature cracking of asphalt-aggregate mixtures. *Transportation Research Record*, No. 1417, pp. 12-20. http://onlinepubs.trb.org/Onlinepubs/trr/1993/1417/1417-002.pdf

Kanerva H. K., Vinson T. S., Zeng H. (1994). Low temperature cracking field validation of the thermal stress restrained specimen test. *SHRP-A-401, National Research Council*, http://onlinepubs.trb.org/onlinepubs/shrp/shrp-a-401.pdf

Pang H. (2006). The development of testing equipment for behavior of asphalt concrete under low temperature and the research on the behavior of asphalt concrete of asphaltic concrete under low temperature [Master Thesis]. *Xi'an: Xi'an University of Technology*.

Sebaaly P. E., Lake A., Epps J. (2002). Evaluation of low-temperature properties of HMA mixtures. *ASCE Journal of Transportation Engineering*, Vol. 128, No. 6, pp. 578-586.

Tan Y. Q., Zhang L., Liu H., Dong Y. M., Xue Z. J. (2010). An evaluation of several kinds of asphalt mixtures' low-temperature performance based on TSRST. *Highway*, No. 1, pp. 171-174.

Tian H. (2012). The study on marshall stability and splitting test of fiber reinforced asphalt mixtures. *Shanxi Science & Technology of Communications*, Vol. 2, No. 1, pp. 9-12.

Tian X. G., Ying R. H., Zheng J. L. (2002). Test on thermal stress in asphalt cement sample and its numerical simulation. *China Civil Engineering Journal*, Vol. 33, No. 3, pp. 25-30. http://doi.org/10.2753/CSH0009-4633350347

Wu X. H., Zhang D. L. (2005). Study of low temperature performance of fiber-enhanced asphalt concrete. *Journal of Highway and Transportation Research and Development*, Vol. 22, No. 2, pp. 7-9. http://doi.org/10.3969/j.issn.1002-0268.2005.02.003

Yin Y. M., Zhang X. N., Zou G. L. (2010). Investigation into low-temperature performance of asphalt mixtures based on glass transition temperature. *Journal of South China University of Technology (Natural Science Edition)*, Vol. 38, No. 10, pp. 89-93. http://doi.org/10.3969/j.issn.1000-565X.2010.10.017

Yu L. S., Xu Q. Y., Wang J. W., Wu L. Y. (2006). Study on behaviors of asphalt concrete under low temperature. *Shui Li Xue Bao*, Vol. 37, No. 5, pp. 634-639.

Zhang D., Xu Y. D., Zhao Y. L. (2009). Method to anti-calculate the parameters in the computing of thermal stress of asphalt pavements based on TSRST. *Petroleum Asphalt*, Vol. 23, No. 5, pp. 30-33. http://doi.org/10.3969/j.issn.1006-7450.2009.05.007

Zhang S. Q., Ying R. H. (2003). Analogue calculation of thermal stress with relaxation effects. *Journal of Changsha Communications Universiy*, Vol. 19, No.1, pp. 31-33. http://doi.org/10.3969/j.issn.1674-599X.2003.01.007